

Reduced-scaling double hybrid DFT with rapid basis set convergence through localized pair natural orbital F12

Nisha Mehta and Jan M. L. Martin*

*Department of Molecular Chemistry and Materials Science, Weizmann Institute of Science,
Rehovot, Israel*

E-mail: gershom@weizmann.ac.il

Phone: +972-8-9342533. Fax: +972-8-9343029

Abstract

Following earlier work [Mehta, N.; Martin, J. M. L. *J. Chem. Theory Comput.* **2022**, *18*, acs.jctc.2c00426] that showed how the slow basis set convergence of double hybrid density functional theory can be obviated by the use of F12 explicit correlation in the GLPT2 step (second order Görling-Levy perturbation theory), we demonstrate here, for the very large and chemically diverse GMTKN55 benchmark suite, that the CPU time scaling of this step can be reduced (asymptotically linearized) using the PNO-L (pair natural orbitals, localized) approximation, at negligible cost in accuracy.

Despite the enormous success of density functional theory (DFT),^{1,2} the exact exchange-correlation functional continues to be elusive, and accurate density functional approximations (DFAs) are highly desirable in computational chemistry. On Perdew’s ‘Jacob’s Ladder’ of DFT,³ the fifth rung corresponds to introducing dependence on unoccupied (virtual) orbitals;

one special case of fifth-rung functionals are double hybrid DFAs.^{4–13} These combine semi-local exchange and correlation from DFT with non-local Fock exchange and GLPT2 (2nd-order Görling-Levy perturbation theory¹⁴) type correlation contributions. Indeed, double hybrid density functionals (DHDFs) are known to be the most accurate DFAs, approaching composite wavefunction theory schemes such as G3 and G4 theories.^{15–17}

Although the basis set convergence of double hybrids is faster than that of wavefunction *ab initio* (WFT) methods, they inherit the slow basis set convergence of MP2 ($\propto L^{-3}$, with L the highest angular momentum in the basis set) to some degree.

WFT basis set convergence can be greatly accelerated by using explicitly correlated methods,^{18–20} in which some geminal terms that explicitly depend on interelectronic distances are added to the one-particle basis set. For instance, Kutzelnigg and Morgan²¹ showed that, for a two-electron system, the singlet-coupled pair correlation energies converge as $\propto L^{-7}$ for explicitly correlated methods, compared to $\propto L^{-3}$ for orbital-only calculations.

While early explicitly correlated WFT studies^{22,23} employed simple r_{12} geminals, the F12 geminal,²⁴ $(1 - \exp \gamma r_{12})/\gamma$, has become the *de facto* standard for explicitly correlated WFT. The introduction of density fitting and auxiliary basis sets sped up integral evaluation to the point F12 calculations became practically feasible.^{25–27}

Practical experience with MP2-F12 and various approximations^{28–31} to CCSD(T)-F12 has shown that, using basis sets specifically developed for F12 calculations,^{32–34} the basis set convergence is drastically faster than for conventional orbital calculations. Thus, F12 approaches have increasingly become a mainstay of high-accuracy WFT; see, for instance, Refs.^{35–45}

We have recently shown,⁴⁶ for the large and chemically diverse GMTKN55 benchmark suite,⁶ that using MP2-F12 in a basis of Kohn-Sham orbitals accelerates basis set convergence of double hybrid DFT to the point that even *spd* basis sets like cc-pVDZ-F12³² are quite close to the basis set limit, and the *spdf* cc-pVTZ-F12³² effectively reaches it.

Nevertheless, two problems remain. First of all, CPU times for the MP2-F12 step scale⁴⁷

as the fifth power of system size (sixth power if F12 amplitudes are optimized in an orbital invariant manner), which will become prohibitive for medium-large systems. Second, in some implementations (such as that in MOLPRO,⁴⁸), F12 methods require a very large amount of scratch storage space, the reading and writing of which creates an I/O bottleneck.

Localized pair natural orbital (PNO-L) WFT approaches such as DLPNO-CCSD(T) of Neese and coworkers,⁴⁹ PNO-CCSD(T) of Werner and coworkers,⁵⁰ and LNO-CCSD(T) of Nagy and Kállay,⁵¹ are gaining increasing acceptance as their size scaling is asymptotically linear; the same can be achieved for MP2 (and in fact this is an intermediate step in the aforementioned calculations). Moreover, when used in tandem with F12 approaches, they combine rapid basis set convergence with gentle system-size scaling, such as in the PNO-MP2-F12 and PNO-CCSD(T)-F12 approaches of Ma and Werner.^{50,52}

It stands to reason that PNO-LMP2-F12 in a basis of Kohn-Sham orbitals might be a robust and computationally efficient way around the scaling and storage bottlenecks of double hybrid DFT (i.e. PNO-DHDF-F12). Assessing the performance of PNO-DHDF-F12 against canonical benchmark results is essential for confirming its robustness. We will show below that when applied to GMTKN55, PNO-DHDF-F12 essentially provides similar accuracy to canonical DHDF-F12, but at much reduced computational cost for large molecules. The latter greatly increases the scope where PNO-DHDF-F12 can be applied.

This study focuses on GMTKN55 database for general main-group thermochemistry, kinetics, and noncovalent interactions. It consists of 55 problem sets comprising 1505 relative energies, which entail 2462 unique single-point energy calculations. These 55 sets can be grouped into five top-level categories: basic properties and reactions of small systems (“Thermo”), reaction energies of large systems and isomerizations (“Large”), barrier heights (“Barrier”), Intermolecular noncovalent interactions (“Intermol”), and intramolecular noncovalent interactions (“Conf”). For more details, see Ref. 6 and references therein.

The performance metric used here, as in Ref. 6 and subsequent studies, e.g., Refs. 7–10,

is the Weighted Total Mean Absolute Deviation (WTMAD2) as defined in Ref. 6:

$$\text{WTMAD2} = \frac{1}{\sum_{i=1}^{55} N_i} \sum_{i=1}^{55} N_i \frac{56.85 \text{ kcal/mol}}{|\overline{\Delta E_i}|} \text{MAD}_i \quad (1)$$

where N_i denotes the number of systems in each test set, $|\overline{\Delta E_i}|$ the mean absolute value of all reference energies from $i=1$ to 55 and MAD_i is the mean absolute deviation of calculated and reference energies. We also consider the decomposition of WTMAD2 into GMTKN55’s five top-level subcategories.

All electronic structure calculations were performed using the MOLPRO2022⁴⁸ package on the Faculty of Chemistry’s HPC cluster “ChemFarm” at the Weizmann Institute of Science. The B2GP-PLYP-D3(BJ) simple double hybrid^{53,54} was considered as a ‘proof of principle’. Computational details in this work largely follow those in our previous study (Ref. 46). All of the KS and PNO-LMP2-F12 steps were performed using density fitting (DF) and the default PNO settings were applied throughout. We considered here the cc-pVnZ-F12 (VnZ-F12 in short),³² augmented versions of these basis sets,³³ and cc-pVnZ-PP-F12³⁴ basis sets for the heavy p-block, where $n=D,T$. Throughout the manuscript PNO-DHDF-F12 refers to DHDF-F12 calculations with the DF-PNO-LMP2-F12. For the CABS (complementary auxiliary basis set),⁵⁵ we used the cc-pVnZ-F12/OptRI auxiliary basis sets;⁵⁶ for Coulomb-exchange (“JK”) fitting, those of Weigend;⁵⁷ finally, for RI-MP2, the MP2FIT sets of Hättig and co-workers.^{58,59} The self-consistent-field (SCF) calculations were carried out with a convergence criterion of $10^{-9} E_h$. All SCF calculations were conducted with MOLPRO’s default integration grid combinations, but with `gridthr` tightened to 10^{-9} . The fixed-amplitude “3C(FIX)” approximation^{24,28} was employed throughout.

In both Ref. 46 and the present work, one subset, C60ISO (isomers of C_{60})⁶⁰ presented insurmountable near-linear dependence problems (overlap matrix elements below 10^{-11}) owing to the p diffuse functions and was eliminated: it anyhow has a small weight in WTMAD2.

We performed PNO-DHDF-F12 calculations with the VnZ-F12 (where $n=D,T$) basis sets.

For six anion-containing subsets AHB21,⁶¹ G21EA,^{62,63} IL16,⁶¹ WATER27,^{64,65} BH76,^{6,63,66,67} and BH76RC,^{6,63} as well as for the RG18⁶ rare-gas clusters, we also considered aug-cc-pVnZ-F12 (n=D,T)³³ or AVnZ-F12 for short; the combination of the latter with VnZ-F12 for the rest of the GMTKN55 suite, we denote VnZ-F12* as in Ref. 46.

For comparison, we also carried out conventional B2GP-PLYP calculations with the commonly used Weigend-Ahlrichs basis sets⁶⁸ def2-TZVPP and def2-QZVPP, as well as with their diffuse-function augmented equivalents⁶⁹ def2-TZVPPD and def2-QZVPPD. Additionally, we considered basis sets of the correlation consistent family:⁷⁰⁻⁷² the shorthand haVnZ (heavy-augmented valence n -tuple zeta, where $n=D,T,Q,5$) stands here for the combination of cc-pVnZ on hydrogen,⁷⁰ aug-cc-pV($n+d$)Z on second-row elements,⁷² aug-cc-pVnZ on first-row⁷¹ and third-row⁷³ elements, and aug-cc-pVnZ-PP on the fourth- and fifth-row p-block elements.⁷⁴⁻⁷⁷ The shorthand VnZ stands for the variant without diffuse functions of this same combo.

The largest basis set for which we were previously able⁴⁶ to obtain fully canonical B2GP-PLYP-F12-D3(BJ) answers, permitting direct comparison, was VQZ-F12*, permitting extrapolation from VTZ-F12* and VQZ-F12*, or for short V{T,Q}Z-F12*.

Table 1’s top pane presents the WTMAD2 for localized PNO-B2GP-PLYP-F12-D3(BJ) for GMTKN55 and its breakdown into the five top-level categories. With the VDZ-F12 basis set, we obtained a WTMAD2 of 3.080 kcal/mol for the GMTKN55 dataset, which goes down insignificantly to 3.073 kcal/mol for VDZ-F12*. Furthermore, VTZ-F12 yields a WTMAD2=3.030 kcal/mol which goes down to 2.961 kcal/mol for the VTZ-F12* variant. We extrapolated VDZ-F12* and VTZ-F12* reaction energies using the two-point extrapolation formula ($A + B/L^\alpha$; L=highest angular momentum present in the basis set) where $\alpha = 3.0878$ for the PT2 components (Table IX in Ref.,⁷⁸ 1st row of lower pane, 2nd column) for the KS component, we just used the highest angular momentum present in the basis set plus the CABS correction. The PNO-B2GP-PLYP-F12-D3(BJ)/V{D,T}Z-F12* level of theory results in WTMAD2 of 2.951 kcal/mol for the entire GMTKN55 database.

WTMAD2 obtained with canonical B2GP-PLYP-F12-D3(BJ) are 2.939, 2.969 and 2.993 kcal/mol, respectively, for VDZ-F12*, VTZ-F12* and V{D,T}Z-F12* (see Ref⁴⁶).

Next (Table 1, middle pane), we explored the basis set convergence of localized B2GP-PLYP-F12-D3(BJ) relative to energies calculated at the canonical B2GP-PLYP-F12-D3(BJ)/V{T,Q}Z-F12* level of theory, which can essentially be regarded as the complete basis set limit. Relative to that, PNO-B2GP-PLYP-F12-D3(BJ) calculations in conjunction with VDZ-F12 and VDZ-F12* provide WTMAD2_{CBS} values of 0.642 and 0.633 kcal/mol, respectively. Increasing the basis set size to VTZ-F12 and VTZ-F12* reduces these deviations to 0.322 and 0.233 kcal/mol, respectively. PNO-B2GP-PLYP-F12-D3(BJ) in conjunction with V{D,T}Z-F12 yields WTMAD2_{CBS}=0.300 kcal/mol. Adding diffuse functions to RG18, WATER27, BH76, BH76RC, AHB21, G21EA and IL16 (i.e. V{D,T}Z-F12*) slightly lowers WTMAD2_{CBS} to 0.262 kcal/mol. WTMAD2_{CBS} values obtained for canonical B2GP-PLYP-F12-D3(BJ) with VDZ-F12*, VTZ-F12* and V{D,T}Z-F12* basis sets are 0.467, 0.207, and 0.215 kcal/mol, respectively (see Ref⁴⁶).

Another angle is offered by considering the WTMAD2 between PNO-B2GP-PLYP-F12-D3(BJ) and canonical B2GP-PLYP-F12-D3(BJ) energies in the same basis set. These can be found in the bottom pane of Table 1. For VDZ-F12, this ‘ Δ WTMAD2_{PNO}’ is 0.513 kcal/mol, most of which is accounted for by the intermolecular and conformational subsets (0.258 and 0.113 kcal/mol, respectively). RG18 alone contributes 0.154 kcal/mol, which together with 0.037 (HEAVY28), 0.024 (S66), and 0.018 (HAL59) accounts for nearly the entire INTERMOL component; CONFOR is mostly due to the four subsets PCONF21 (0.026), BUT14DIOL (0.025), Amino20x4 (0.024), and MCONF (0.019 kcal/mol). Essentially the same picture emerges for VDZ-F12*. For VTZ-F12, the ‘PNO Δ WTMAD2’ is 0.333 kcal/mol, the largest two contributor sets being RG18 and HEAVY28 at 0.094 and 0.038 kcal/mol, respectively; in the VTZ-F12* variant, the RG18 contribution drops to 0.029 kcal/mol. Similar accuracy is found for V{D,T}Z-F12 and V{D,T}Z-F12* extrapolations, in each case RG18 being again the largest contributor.

We shall now briefly compare the computational cost of localized (denoted PNO-F12 for short in the tables) and canonical B2GP-PLYP-F12-D3(BJ) calculations. This is perhaps best illustrated by considering timings for the linear n-alkane dimers as a function of n ; we considered first (ethane)₂ through (n-heptane)₂ which make up the ADIM6^{6,79} subset of GMTKN55, then we extended this series for $n = 8$ through $n = 24$ by manually inserting CH₂ groups (since we were only interested in timings, optimized structures were not deemed necessary). All calculations in this comparison are run on identical hardware, namely Intel(R) Haswell 2.40 GHz, 16 cores, 256 GB RAM, and 3.6TB of fast striped SSDs. Detailed single-core and 16-core timings for both F12 and orbital-only calculations, with various basis sets, can be found in the Supporting Information; in Table 2 we report values relative to PNO-F12/VDZ-F12=1.00. As we have seen above, localized PNO-B2GP-PLYP-F12/VDZ-F12 yields results of comparable quality to canonical B2GP-PLYP-F12/VDZ-F12. The localized PNO-B2GP-PLYP-F12/VDZ-F12 are comparable in cost to their canonical counterparts for n-butane dimer, but as the chain length grows, the gap opens up, to the point where for (n-hexadecane)₂ the PNO calculation is almost 18 times faster than its canonical counterpart. The cost for PNO-B2GP-PLYP-F12/VTZ-F12 is an almost constant factor of 3.5-3.6 greater than for the same calculation in the smaller VDZ-F12 basis set, meaning that for n-decane dimer — the largest case for which we were able to do the canonical F12/VTZ-F12 calculation — the latter took about 6 times as long as its PNO counterpart. When comparing with B2GP-PLYP/haV{T,Q}Z, PNO-B2GP-PLYP-F12/VDZ-F12 goes from about 2 times to about 7 times faster as the chains grow longer, and for def2-{T,Q}ZVPPD from 2 to 5 times faster. The B2GP-PLYP/haV{Q,5}Z calculations range from about 9 times longer than PNO-B2GP-PLYP-F12/VDZ-F12 for butane dimer, to about 27 times as long for (n-hexadecane)₂.

In fact, a power law fit to the total computational time for n-heptane through n-hexadecane dimers, (C_nH_{n+2})₂ ($n=7-10, 12, 14, 16$, see the Table of Contents graphic), reveals $\propto n^{4.88}$ scaling (nearly the expected $\propto n^5$) for canonical B2GP-PLYP-F12-D3(BJ), but approximate

$\propto n^{2.58}$ scaling for PNO-B2GP-PLYP-F12-D3(BJ).

For mass storage requirements, the ratios are even more lopsided (see Table S1 in the Supporting Information): the PNO-F12 calculation on n-butane dimer requires only one-tenth the scratch space of its canonical counterpart, and for n-hexadecane this drops to one-eighteenth. These ratios are pretty much independent of the basis set. What this means in concrete terms: for n-hexadecane dimer with the VDZ-F12 basis set, the canonical calculation requires almost 3.5 TB of scratch space, versus about 196 GB for the PNO calculation. On our cluster, this makes the difference between having to run the calculation on a dedicated ‘heavyio’ node with a large local scratch SSD, and being able to run it on any available general-purpose node.

However, for larger systems, CPU time scaling of the PNO-GLPT2-F12 step in PNO-B2GP-PLYP-F12-D3(BJ) becomes even gentler. Figure 1 illustrates this for dimers of parallel chains of n-alkanes through $n=24$ (tetraicosane dimer) with the cc-pVDZ-F12 and cc-pVTZ-F12 basis sets. The canonical calculations were only feasible through $n=16$ (for which the PT2-F12 step required 3.5TB of scratch space): a power law fit of CPU times for the PT2-F12 step reveals an almost perfect $\propto n^5$ dependence ($R^2 = 0.9999$), as will the total CPU time which is completely dominated by this step. For PNO-B2GP-PLYP-F12-D3(BJ)/cc-pVDZ-F12, a power law fit for $n = 8$ through $n = 24$ reveals a much gentler $\propto n^{2.64}$ scaling ($R^2 = 0.9997$): a component breakdown of the times reveals an approximately $\propto n^3$ scaling for the Kohn-Sham step ($R^2 = 0.998$) paired with a scaling for the PNO-PT2-F12 step that follows a roughly $\propto n^{2.16}$ power law ($R^2 = 0.997$), but hews more closely ($R^2 = 0.9997$) to a quadratic fit. Largely the same trends are found for cc-pVTZ-F12 (see the Excel sheet in Supporting Information).

When running in a more realistic fashion on 16 cores, we find speedups by about a factor of 8 for B2GP-PLYP-F12-D3(BJ), and of 12 for PNO-B2GP-PLYP-F12-D3(BJ). More detailed scrutiny reveals that, while in the former case the scaling is determined by the PT2-F12 step (where I/O bandwidth limitations place a practical limit on parallelism), in the

Table 1: Statistical analysis (kcal/mol) of the basis set convergence in localized B2GP-PLYP-F12-D3(BJ) calculations for the GMTKN55 database and its categories.

relative to the Ref. ⁶ reference data						
	WTMAD2	THERMO	BARRIERS	LARGE	CONF	INTERMOL
VDZ-F12	3.080	0.590	0.327	0.662	0.636	0.864
VDZ-F12 ^{*a}	3.073	0.583	0.325	0.662	0.636	0.867
VTZ-F12	3.030	0.590	0.324	0.659	0.599	0.858
VTZ-F12 ^{*a}	2.961	0.587	0.322	0.659	0.599	0.794
V{D,T}Z-F12	3.025	0.588	0.327	0.655	0.593	0.863
V{D,T}Z-F12 ^{*a}	2.951	0.586	0.324	0.655	0.593	0.793
relative to the B2GP-PLYP-F12-D3(BJ)/V{T,Q}Z-F12* basis set limit						
VDZ-F12	0.642	0.086	0.052	0.093	0.135	0.277
VDZ-F12 ^{*a}	0.633	0.074	0.048	0.093	0.135	0.284
VTZ-F12	0.322	0.032	0.019	0.033	0.057	0.182
VTZ-F12 ^{*a}	0.233	0.023	0.017	0.033	0.057	0.103
V{D,T}Z-F12	0.300	0.033	0.023	0.033	0.048	0.163
V{D,T}Z-F12 ^{*a}	0.262	0.026	0.021	0.033	0.048	0.134
relative to canonical B2GP-PLYP-F12-D3(BJ) in the same basis set						
VDZ-F12	0.513	0.046	0.034	0.062	0.113	0.258
VDZ-F12 [*]	0.525	0.045	0.032	0.062	0.113	0.273
VTZ-F12	0.333	0.024	0.017	0.038	0.066	0.188
VTZ-F12 [*]	0.269	0.024	0.018	0.038	0.066	0.123
V{D,T}Z-F12	0.335	0.023	0.018	0.041	0.073	0.180
V{D,T}Z-F12 [*]	0.317	0.023	0.020	0.041	0.073	0.161

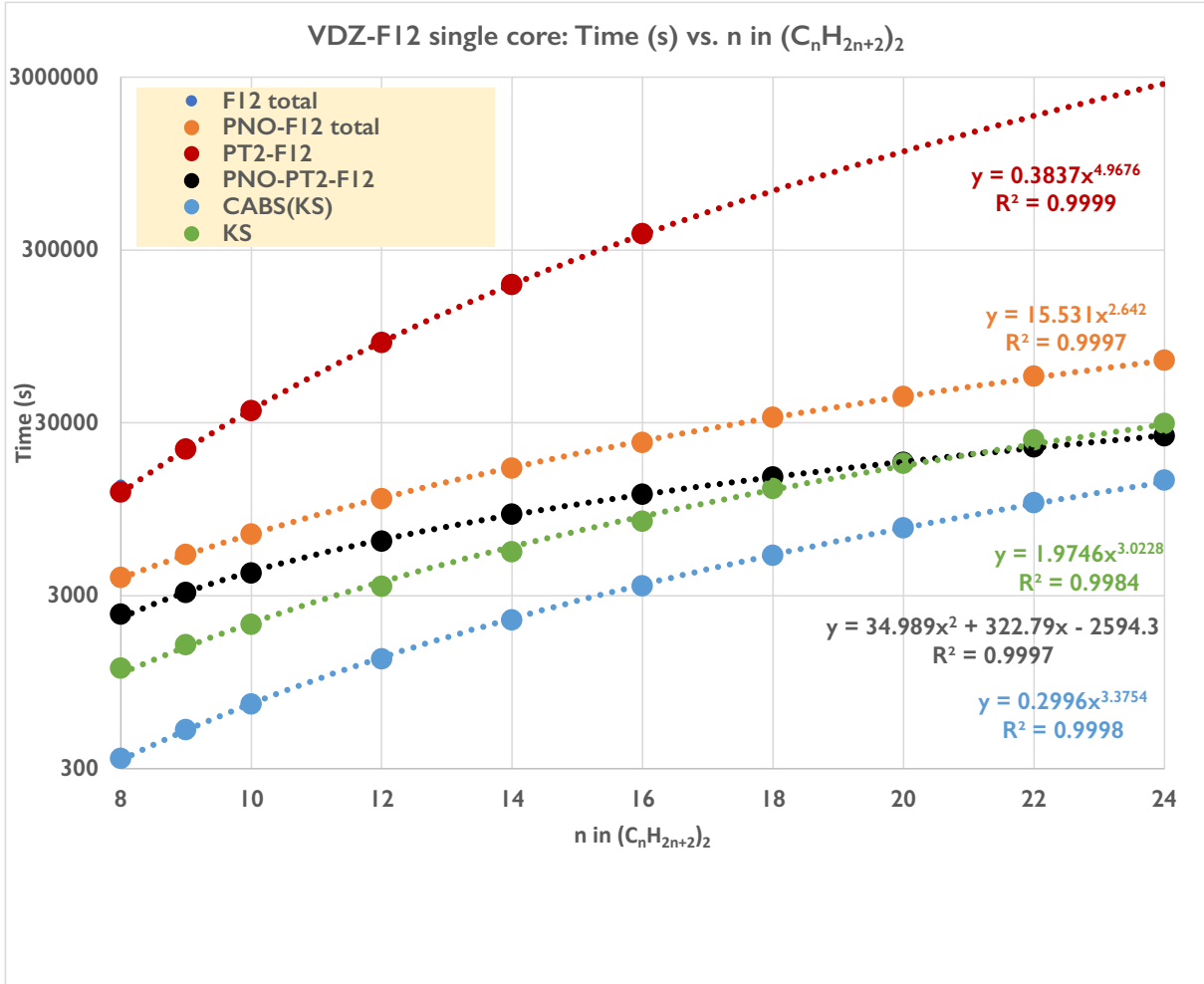
^aVnZ-F12 (where n=D,T) basis set was used for Ne-containing systems in RG18 due to numerical problems.

Table 2: Relative wall-clock times for the PNO-B2GP-PLYP-F12, B2GP-PLYP-F12 and B2GP-PLYP calculations for $(C_nH_{n+2})_2$. All timings on a single Intel Haswell 2.4GHz core in 256 GB RAM and with 3.6TB striped solid state scratch disk. Timing is shown relative to PNO-B2GP-PLYP-F12/VDZ-F12

	B2GP-PLYP-F12		B2GP-PLYP						B2GP-PLYP-F12	
	PNO-F12	canonical							PNO-F12	canonical
	VDZ-F12	VDZ-F12	{T,Q}ZVPP	{T,Q}ZVPPD	V{T,Q}Z	haV{T,Q}Z	haV{Q,5}Z	AV{T,Q}Z	VTZ-F12	VTZ-F12
(butane) ₂	1.00	1.20	1.10	1.77	1.90	2.22	8.61	4.18	3.50	4.22
(pentane) ₂	1.00	1.58	1.10	1.82	1.43	2.34	9.18	4.38	3.52	5.79
(hexane) ₂	1.00	2.05	1.18	1.96	1.50	2.53	10.13	4.72	3.57	7.94
(heptane) ₂	1.00	2.61	1.24	2.12	1.60	2.74	11.06	5.12	3.62	10.26
(n-octane) ₂	1.00	3.52	1.35	2.33	1.72	2.99	12.08	5.56	3.63	13.57
(n-nonane) ₂	1.00	4.52	1.46	2.53	1.87	3.27	13.36	6.06	3.63	17.40
(n-decane) ₂	1.00	5.70	1.61	2.81	2.04	3.60	14.81	6.61	3.64	21.87
(n-dodecane) ₂	1.00	8.71	1.95	3.42	2.46	4.31	18.22	7.98	3.67	
(n-tetradecane) ₂	1.00	12.39	2.49	4.11	2.95	5.94	23.59	11.27	3.60	
(n-hexadecane) ₂	1.00	17.60	2.85	5.02	3.48	6.62	27.35	11.31	3.64	

Timings for extrapolated B2GP-PLYP/{T,Q}ZVPP and the like correspond to the sum of TZVPP and QZVPP, and so forth.

Figure 1: Elapsed times (s, logarithmic scale) of canonical GLPT2-F12 and localized PNO-GLPT2-F12 steps of $(C_nH_{2n+2})_2$ on a single Intel Skylake E5-2630 v3 core at 2.4 GHz, with 256 GB RAM and 3.6TB striped SSD



Note that, for the conventional B2GP-PLYP-F12-D3(BJ)/cc-pVDZ-F12 calculation, the PT2-F12 step dominates the CPU time to such an extent that the ‘F12 total’ line is obscured by the crimson ‘PT2-F12’ line. KS is the time spent in the Kohn-Sham iterations; CABS(KS) that for the evaluation of the CABS correction; PT2-F12 and PNO-PT2-F12 refers to the canonical and PNO perturbation theory steps, respectively; ‘F12 total’ is the time for the entire canonical calculation; and ‘PNO-F12 total’ that for the entire localized calculation.

latter case PNO-PT2-F12 actually parallelizes close to ideally and the Kohn-Sham step is the parallelization efficiency-limiting factor. At the end of the day, parallelization additionally favors PNO-B2GP-PLYP-F12-D3(BJ) and makes it an even more attractive method.

Now would we be able to realize similar gains from PNO-LMP2 in orbital-only (i.e., non-F12) calculations? We have considered this for haVTZ and haVQZ basis sets along the same

n-alkane dimer series for $n=8-16$, parallel on 16 cores; the timing data and their breakdown can again be found in the Supporting Information. For low n , the PNO approach is actually slightly costlier, but for $n=16$ we can see a reduction in total CPU time by about 25%. Needless to say, this does not even come close to the order-of-magnitude or more that can be saved in PNO-F12 vs. canonical F12 double hybrids. (We note that in the orbital-only calculations, the KS step accounts for the lion’s share of the total time, although this will eventually be reversed as chains grow still longer.)

The principal conclusion of this work is that double hybrid F12 calculations, which largely eliminate the slow basis set convergence of double hybrids, can be carried out without significant loss of accuracy using localized pair natural orbitals in the F12 step. Thus, CPU and mass storage requirements scale much more gently with system size, making the method amenable also to, and promising for, larger systems.

Acknowledgement

Work on this paper was supported by the Israel Science Foundation (grant 1969/20), by the Minerva Foundation (grant 2020/05), and by a research grant from the Artificial Intelligence and Smart Materials Research Fund (in memory of Dr. Uriel Arnon), Israel. The authors would like to thank Golokesh Santra for helpful comments on the draft manuscript, and Emmanouil Semidalas for proofreading the revised manuscript.

Supporting Information Available

The Supporting Information is available free of charge at <http://doi.org/10.1021/jz-2022-02620q>. It consists of a Microsoft Excel workbook containing statistical results of all assessed methods, as well as a sample MOLPRO input file for PNO-B2GP-PLYP-F12 and 1-core and 16-core timing data for the n-alkane dimer series, using different approaches, and broken down by calculation step.

References

- (1) Hohenberg, P.; Kohn, W. Inhomogeneous electron gas. *Phys. Rev.* **1964**, *136*, B864.
- (2) Kohn, W.; Sham, L. J. Self-consistent equations including exchange and correlation effects. *Phys. Rev.* **1965**, *140*, A1133–A1138.
- (3) Perdew, J. P.; Schmidt, K. Jacob’s ladder of density functional approximations for the exchange-correlation energy. *AIP Conf. Proc.* **2001**, *577*, 1–20.
- (4) Grimme, S. Semiempirical hybrid density functional with perturbative second-order correlation. *J. Chem. Phys.* **2006**, *124*, 034108.
- (5) Goerigk, L.; Grimme, S. Double-Hybrid Density Functionals. *Wiley Interdiscip. Rev.: Comput. Mol. Sci.* **2014**, *4*, 576–600.
- (6) Goerigk, L.; Hansen, A.; Bauer, C.; Ehrlich, S.; Najibi, A.; Grimme, S. A look at the density functional theory zoo with the advanced GMTKN55 database for general main group thermochemistry, kinetics and noncovalent interactions. *Phys. Chem. Chem. Phys.* **2017**, *19*, 32184–32215.
- (7) Goerigk, L.; Mehta, N. A trip to the density functional theory zoo: warnings and recommendations for the user. *Aust. J. Chem.* **2019**, *72*, 563–573.
- (8) Santra, G.; Sylvetsky, N.; Martin, J. M. L. Minimally empirical double-hybrid functionals trained against the GMTKN55 database: revDSD-PBEP86-D4, revDOD-PBE-D4, and DOD-SCAN-D4. *J. Phys. Chem. A* **2019**, *123*, 5129–5143.
- (9) Mehta, N.; Casanova-Páez, M.; Goerigk, L. Semi-empirical or non-empirical double-hybrid density functionals: which are more robust? *Phys. Chem. Chem. Phys.* **2018**, *20*, 23175–23194.
- (10) Martin, J. M. L.; Santra, G. Empirical double-hybrid density functional theory: A ‘third way’ in between WFT and DFT. *Isr. J. Chem.* **2020**, *60*, 787–804.

- (11) Mardirossian, N.; Head-Gordon, M. Survival of the most transferable at the top of Jacob’s ladder: defining and testing the ω B97M(2) double hybrid density functional. *J. Chem. Phys.* **2018**, *148*, 241736.
- (12) Brémond, E.; Ciofini, I.; Sancho-García, J. C.; Adamo, C. Nonempirical Double-Hybrid Functionals: An Effective Tool for Chemists. *Acc. Chem. Res.* **2016**, *49*, 1503–1513.
- (13) Zhang, I. Y.; Xu, X. Doubly hybrid density functional for accurate description of thermochemistry, thermochemical kinetics and nonbonded interactions. *Int. Rev. Phys. Chem.* **2011**, *30*, 115–160.
- (14) Görling, A.; Levy, M. Exact Kohn-Sham scheme based on perturbation theory. *Phys. Rev. A* **1994**, *50*, 196–204.
- (15) Curtiss, L. A.; Raghavachari, K.; Redfern, P. C.; Rassolov, V.; Pople, J. A. Gaussian-3 (G3) theory for molecules containing first and second-row atoms. *J. Chem. Phys.* **1998**, *109*, 7764–7776.
- (16) Curtiss, L. A.; Redfern, P. C.; Raghavachari, K. Gaussian-4 theory. *J. Chem. Phys.* **2007**, *126*, 084108.
- (17) Curtiss, L. A.; Redfern, P. C.; Raghavachari, K. Gn theory. *Wiley Interdiscip. Rev. Comput. Mol. Sci.* **2011**, *1*, 810–825.
- (18) Hättig, C.; Klopper, W.; Köhn, A.; Tew, D. P. Explicitly correlated electrons in molecules. *Chem. Rev.* **2012**, *112*, 4–74.
- (19) Kong, L.; Bischoff, F. A.; Valeev, E. F. Explicitly correlated R12/F12 methods for electronic structure. *Chem. Rev.* **2012**, *112*, 75–107.
- (20) Ten-no, S.; Noga, J. Explicitly correlated electronic structure theory from R12/F12 ansätze. *Wiley Interdiscip. Rev. Comput. Mol. Sci.* **2012**, *2*, 114–125.

- (21) Kutzelnigg, W.; Morgan III, J. D. Rates of convergence of the partial-wave expansions of atomic correlation energies. *J. Chem. Phys.* **1992**, *96*, 4484–4508.
- (22) Klopper, W.; Kutzelnigg, W. Møller-Plesset calculations taking care of the correlation cusp. *Chem. Phys. Lett* **1987**, *134*, 17–22.
- (23) Kutzelnigg, W.; Klopper, W. Wave functions with terms linear in the interelectronic coordinates to take care of the correlation cusp. I. General theory. *J. Chem. Phys.* **1991**, *94*, 1985–2001.
- (24) Ten-no, S. Initiation of explicitly correlated Slater-type geminal theory. *Chem. Phys. Lett.* **2004**, *398*, 56–61.
- (25) Klopper, W.; Samson, C. C. M. Explicitly correlated second-order Møller-Plesset methods with auxiliary basis sets. *J. Chem. Phys.* **2002**, *116*, 6397–6410.
- (26) Manby, F. R. Density fitting in second-order linear-r12 Møller-Plesset perturbation theory. *J. Chem. Phys.* **2003**, *119*, 4607–4613.
- (27) May, A. J.; Valeev, E.; Polly, R.; Manby, F. R. Analysis of the errors in explicitly correlated electronic structure theory. *Phys. Chem. Chem. Phys.* **2005**, *7*, 2710–2713.
- (28) Werner, H.-J.; Adler, T. B.; Manby, F. R. General orbital invariant MP2-F12 theory. *J. Chem. Phys.* **2007**, *126*, 164102.
- (29) Valeev, E. F. Coupled-cluster methods with perturbative inclusion of explicitly correlated terms: A preliminary investigation. *Phys. Chem. Chem. Phys.* **2008**, *10*, 106–113.
- (30) Valeev, E. F.; Crawford, T. D. Simple coupled-cluster singles and doubles method with perturbative inclusion of triples and explicitly correlated geminals: The CCSD(T)R12 model. *J. Chem. Phys.* **2008**, *128*, 244113.

- (31) Hättig, C.; Tew, D. P.; Köhn, A. Communications: Accurate and efficient approximations to explicitly correlated coupled-cluster singles and doubles, CCSD-F12. *J. Chem. Phys.* **2010**, *132*, 231102.
- (32) Peterson, K. A.; Adler, T. B.; Werner, H.-J. Systematically convergent basis sets for explicitly correlated wavefunctions: The atoms H, He, B–Ne, and Al–Ar. *J. Chem. Phys.* **2008**, *128*, 084102.
- (33) Sylvetsky, N.; Kesharwani, M. K.; Martin, J. M. L. The aug-cc-pVnZ-F12 basis set family: Correlation consistent basis sets for explicitly correlated benchmark calculations on anions and noncovalent complexes. *J. Chem. Phys.* **2017**, *147*, 134106.
- (34) Hill, J. G.; Peterson, K. A. Correlation consistent basis sets for explicitly correlated wavefunctions: Pseudopotential-based basis sets for the post-d main group elements Ga–Rn. *J. Chem. Phys.* **2014**, *141*, 094106.
- (35) Marchetti, O.; Werner, H.-J. Accurate calculations of intermolecular interaction energies using explicitly correlated coupled cluster wave functions and a dispersion-weighted MP2 method. *J. Phys. Chem. A* **2009**, *113*, 11580–11585.
- (36) Peterson, K. A.; Dixon, D. A.; Stoll, H. The Use of Explicitly Correlated Methods on XeF₆ Predicts a C_{3v} Minimum with a Sterically Active, Free Valence Electron Pair on Xe. *J. Phys. Chem. A* **2012**, *116*, 9777–9782.
- (37) Pavošević, F.; Pinski, P.; Riplinger, C.; Neese, F.; Valeev, E. F. SparseMaps—A systematic infrastructure for reduced-scaling electronic structure methods. IV. Linear-scaling second-order explicitly correlated energy with pair natural orbitals. *J. Chem. Phys.* **2016**, *144*, 144109.
- (38) Karton, A.; Martin, J. M. L. Explicitly correlated Wn theory: W1-F12 and W2-F12. *J. Chem. Phys.* **2012**, *136*, 124114.

- (39) Peterson, K. A.; Kesharwani, M. K.; Martin, J. M. L. The cc-pV5Z-F12 basis set: reaching the basis set limit in explicitly correlated calculations. *Mol. Phys.* **2015**, *113*, 1551–1558.
- (40) Sylvetsky, N.; Peterson, K. A.; Karton, A.; Martin, J. M. L. Toward a W4-F12 approach: Can explicitly correlated and orbital-based ab initio CCSD(T) limits be reconciled? *J. Chem. Phys.* **2016**, *144*, 214101.
- (41) Brauer, B.; Kesharwani, M. K.; Martin, J. M. L. Some observations on counterpoise corrections for explicitly correlated calculations on noncovalent interactions. *J. Chem. Theory Comput.* **2014**, *10*, 3791–3799.
- (42) Fogueri, U. R.; Kozuch, S.; Karton, A.; Martin, J. M. L. The melatonin conformer space: benchmark and assessment of wave function and DFT methods for a paradigmatic biological and pharmacological molecule. *J. Phys. Chem. A* **2013**, *117*, 2269–77.
- (43) Brauer, B.; Kesharwani, M. K.; Kozuch, S.; Martin, J. M. L. The S66x8 benchmark for noncovalent interactions revisited: explicitly correlated ab initio methods and density functional theory. *Phys. Chem. Chem. Phys.* **2016**, *18*, 20905–20925.
- (44) Manna, D.; Kesharwani, M. K.; Sylvetsky, N.; Martin, J. M. L. Conventional and Explicitly Correlated ab Initio Benchmark Study on Water Clusters: Revision of the BEGDB and WATER27 Data Sets. *J. Chem. Theory Comput.* **2017**, *13*, 3136–3152.
- (45) Kesharwani, M. K.; Manna, D.; Sylvetsky, N.; Martin, J. M. L. The X40×10 Halogen Bonding Benchmark Revisited: Surprising Importance of (n–1)d Subvalence Correlation. *J. Phys. Chem. A* **2018**, *122*, 2184–2197.
- (46) Mehta, N.; Martin, J. M. L. Explicitly correlated double hybrid DFT: a comprehensive analysis of the basis set convergence on the GMTKN55 database. *J. Chem. Theory Comput.* **2022**, *18*, 10.1021/acs.jctc.2c00426.

- (47) Bachorz, R. A.; Bischoff, F. A.; Glöck, A.; Hättig, C.; Höfener, S.; Klopper, W.; Tew, D. P. The MP2-F12 method in the TURBOMOLE program package. *J. Comput. Chem.* **2011**, *32*, 2492–2513.
- (48) Werner, H.-J.; Knowles, P. J.; Manby, F. R.; Black, J. A.; Doll, K.; Heßelmann, A.; Kats, D.; Köhn, A.; Korona, T.; Kreplin, D. A., et al. The Molpro quantum chemistry package. *J. Chem. Phys.* **2020**, *152*, 144107.
- (49) Riplinger, C.; Sandhoefer, B.; Hansen, A.; Neese, F. Natural Triple Excitations in Local Coupled Cluster Calculations with Pair Natural Orbitals. *J. Chem. Phys.* **2013**, *139*, 134101.
- (50) Ma, Q.; Werner, H.-J. Explicitly correlated local coupled-cluster methods using pair natural orbitals. *Wiley Interdiscip. Rev. Comput. Mol. Sci.* **2018**, *8*, e1371.
- (51) Nagy, P. R.; Kállay, M. Approaching the Basis Set Limit of CCSD(T) Energies for Large Molecules with Local Natural Orbital Coupled-Cluster Methods. *J. Chem. Theory Comput.* **2019**, *15*, 5275–5298.
- (52) Ma, Q.; Werner, H.-J. Scalable Electron Correlation Methods. 2. Parallel PNO-LMP2-F12 with Near Linear Scaling in the Molecular Size. *J. Chem. Theory Comput.* **2015**, *11*, 5291–5304.
- (53) Karton, A.; Tarnopolsky, A.; Lamère, J.-F.; Schatz, G. C.; Martin, J. M. L. Highly accurate first-principles benchmark data sets for the parametrization and validation of density functional and other approximate methods. Derivation of a robust, generally applicable, double-hybrid functional for thermochemistry and thermochemical kinetics. *J. Phys. Chem. A* **2008**, *112*, 12868–12886.
- (54) Goerigk, L.; Grimme, S. A thorough benchmark of density functional methods for general main group thermochemistry, kinetics, and noncovalent interactions. *Phys. Chem. Chem. Phys.* **2011**, *13*, 6670–6688.

- (55) Valeev, E. F. Improving on the resolution of the identity in linear R12 ab initio theories. *Chem. Phys. Lett* **2004**, *395*, 190–195.
- (56) Yousaf, K. E.; Peterson, K. A. Optimized complementary auxiliary basis sets for explicitly correlated methods: aug-cc-pVnZ orbital basis sets. *Chem. Phys. Lett* **2009**, *476*, 303–307.
- (57) Weigend, F. A fully direct RI-HF algorithm: Implementation, optimised auxiliary basis sets, demonstration of accuracy and efficiency. *Phys. Chem. Chem. Phys.* **2002**, *4*, 4285–4291.
- (58) Weigend, F.; Köhn, A.; Hättig, C. Efficient use of the correlation consistent basis sets in resolution of the identity MP2 calculations. *J. Chem. Phys.* **2002**, *116*, 3175–3183.
- (59) Hättig, C. Optimization of auxiliary basis sets for RI-MP2 and RI-CC2 calculations: Core–valence and quintuple- ζ basis sets for H to Ar and QZVPP basis sets for Li to Kr. *Phys. Chem. Chem. Phys.* **2005**, *7*, 59–66.
- (60) Sure, R.; Hansen, A.; Schwerdtfeger, P.; Grimme, S. Comprehensive theoretical study of all 1812 C₆₀ isomers. *Phys. Chem. Chem. Phys.* **2017**, *19*, 14296–14305.
- (61) Lao, K. U.; Schäffer, R.; Jansen, G.; Herbert, J. M. Accurate Description of Intermolecular Interactions Involving Ions Using Symmetry-Adapted Perturbation Theory. *J. Chem. Theory Comput.* **2015**, *11*, 2473–2486.
- (62) Curtiss, L. A.; Raghavachari, K.; Trucks, G. W.; Pople, J. A. Gaussian-2 theory for molecular energies of first-and second-row compounds. *J. Chem. Phys.* **1991**, *94*, 7221–7230.
- (63) Goerigk, L.; Grimme, S. A General Database for Main Group Thermochemistry, Kinetics, and Noncovalent Interactions - Assessment of Common and Reparameterized (Meta-)GGA Density Functionals. *J. Chem. Theory Comput.* **2010**, *6*, 107–126.

- (64) Bryantsev, V.; Diallo, M.; van Duin, A.; Goddard, W. Evaluation of B3LYP, X3LYP, and M06-Class Density Functionals for Predicting the Binding Energies of Neutral, Protonated, and Deprotonated Water Clusters. *J. Chem. Theory Comput.* **2009**, *5*, 1016–1026.
- (65) Manna, D.; Kesharwani, M. K.; Sylvetsky, N.; Martin, J. M. L. Conventional and Explicitly Correlated ab Initio Benchmark Study on Water Clusters: Revision of the BEGDB and WATER27 Data Sets. *J. Chem. Theory Comput.* **2017**, *13*, 3136–3152.
- (66) Zhao, Y.; Lynch, B. J.; Truhlar, D. G. Multi-coefficient extrapolated density functional theory for thermochemistry and thermochemical kinetics. *Phys. Chem. Chem. Phys.* **2005**, *7*, 43–52.
- (67) Friedrich, J.; Hänchen, J. Incremental CCSD(T)(F12*)|MP2: A Black Box Method To Obtain Highly Accurate Reaction Energies. *J. Chem. Theory Comput.* **2013**, *9*, 5381–5394.
- (68) Weigend, F.; Ahlrichs, R. Balanced basis sets of split valence, triple zeta valence and quadruple zeta valence quality for H to Rn: Design and assessment of accuracy. *Phys. Chem. Chem. Phys.* **2005**, *7*, 3297–3305.
- (69) Rappoport, D.; Furche, F. Property-optimized Gaussian basis sets for molecular response calculations. *J. Chem. Phys.* **2010**, *133*, 134105.
- (70) Dunning Jr, T. H. Gaussian basis sets for use in correlated molecular calculations. I. The atoms boron through neon and hydrogen. *J. Chem. Phys.* **1989**, *90*, 1007–1023.
- (71) Kendall, R. A.; Dunning Jr, T. H.; Harrison, R. J. Electron affinities of the first-row atoms revisited. Systematic basis sets and wave functions. *J. Chem. Phys.* **1992**, *96*, 6796–6806.

- (72) Dunning Jr, T. H.; Peterson, K. A.; Wilson, A. K. Gaussian basis sets for use in correlated molecular calculations. X. The atoms aluminum through argon revisited. *J. Chem. Phys.* **2001**, *114*, 9244–9253.
- (73) Wilson, A. K.; Woon, D. E.; Peterson, K. A.; Dunning, T. H. Gaussian basis sets for use in correlated molecular calculations. IX. The atoms gallium through krypton. *J. Chem. Phys.* **1999**, *110*, 7667–7676.
- (74) Metz, B.; Stoll, H.; Dolg, M. Small-core multiconfiguration-Dirac-Hartree-Fock-adjusted pseudopotentials for post-*d* main group elements: Application to PbH and PbO. *J. Chem. Phys.* **2000**, *113*, 2563–2569.
- (75) Peterson, K. A. Systematically convergent basis sets with relativistic pseudopotentials. I. Correlation consistent basis sets for the post-*d* group 13–15 elements. *J. Chem. Phys.* **2003**, *119*, 11099–11112.
- (76) Peterson, K. A.; Figgen, D.; Goll, E.; Stoll, H.; Dolg, M. Systematically convergent basis sets with relativistic pseudopotentials. II. Small-core pseudopotentials and correlation consistent basis sets for the post-*d* group 16–18 elements. *J. Chem. Phys.* **2003**, *119*, 11113–11123.
- (77) Peterson, K. A.; Shepler, B. C.; Figgen, D.; Stoll, H. On the Spectroscopic and Thermochemical Properties of ClO, BrO, IO, and Their Anions. *J. Phys. Chem. A* **2006**, *110*, 13877–13883.
- (78) Hill, J. G.; Peterson, K. A.; Knizia, G.; Werner, H.-J. Extrapolating MP2 and CCSD explicitly correlated correlation energies to the complete basis set limit with first and second row correlation consistent basis sets. *J. Chem. Phys.* **2009**, *131*, 194105.
- (79) Grimme, S.; Antony, J.; Ehrlich, S.; Krieg, H. A consistent and accurate ab initio parametrization of density functional dispersion correction (DFT-D) for the 94 elements H-Pu. *J. Chem. Phys.* **2010**, *132*, 154104.

Graphical TOC Entry

